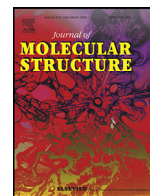




Contents lists available at ScienceDirect

Journal of Molecular Structure

journal homepage: www.elsevier.com/locate/molstr

Cytotoxic activity and apoptosis induction by a series Ag(I)-NHC complexes on human breast cancer cells and non-tumorigenic epithelial cell line

Türkan Kutlu^a, Işıl Yıldırım^{b,c,*}, Hande Karabıyık^d, Ayten Kılınçlı^e, İbrahim Tekedereli^e, Yetkin Gök^f, Miriş Dikmen^g, Aydın Aktaş^{f,h}

^a Department of Chemistry/Biochemistry, Faculty of Science, Inonu University, Malatya 44280, Turkey

^b Science Institute, Inonu University, Malatya 44280, Turkey

^c Vocational School, Pharmacy Services Program, Beykent University, Istanbul 34500, Turkey

^d Department of Physics, Faculty of Science, Dokuz Eylül University, Izmir 35390, Turkey

^e Department of Medical Biology and Genetics, Medical School, Inonu University, Malatya 44280, Turkey

^f Department of Chemistry/Organic Chemistry, Faculty of Science, Inonu University, Malatya 44280, Turkey

^g Department of Pharmacology, Faculty of Pharmacy, Anadolu University, Eskisehir 26210, Turkey

^h Health Services Vocational School, Inonu University, Malatya 44280, Turkey

ARTICLE INFO

Article history:

Received 5 September 2020

Revised 12 October 2020

Accepted 14 October 2020

Available online xxx

Keyword:

Ag(I)-NHC

Morpholine

Benzimidazolium

XRD

MCF7

MDA-MB-231

MCF10A

Apoptosis

Flow cytometry

ABSTRACT

The main problems encountered in treatment with anticancer drugs, undesired side effects, and toxicity. One of the most important parameters in cell transport is the lipophilic and solubility property of the drug. Enough with the potential effects, side effects with minimal demand for new anticancer compounds, mechanisms of action of the compound can meet because of increased efforts to be clarified. In this case, scientists were encouraged to do new research. In particular, the organometallic compounds are one of the topics focused lately. Ag(I)-NHC complexes are one of the most important classes of organometallic compounds. Although the anticancer activity of Ag(I)-NHC complexes have been known recently times, the anticancer effects of 2-morpholino ethyl substituted benzimidazolium derivative, lipophilic, and solubility properties. Ag(I)-NHC complexes have not unknown yet. Therefore, we aimed to investigate of cytotoxic effect and apoptosis mechanism on breast cancer cell lines (MCF7), breast adenocarcinoma cell lines (MDA-MB-231), and non-tumorigenic epithelium cell lines (MCF 10A) of new Ag(I)-NHC complexes that derivative from morpholine-linked benzimidazole, were synthesized and antimicrobial activity was determined in our previous study. The cytotoxicity was determined by the MTS method, and the apoptosis mechanisms were determined the cell cycle, Annexin V, and caspase-3 analysis. A new benzimidazolium salt bearing morpholino ethyl substituent (**2**) was synthesized. This benzimidazolium salt was characterized by NMR and FT-IR spectroscopic method and elemental analysis technique. Also, the structure of the new benzimidazolium salt was confirmed by single-crystal X-ray diffraction. Ag(I)-NHC complexes inhibited the growth of MCF7 and MDA-MB-231 cells depending on the dosage and time. The complexes **3a** and **3b** exhibited a significant difference $p < 0.05$; $p < 0.001$; and $p < 0.001$ level depend on depending on the increase in concentration on cancer cells. All compound induced by apoptosis was associated with stopping the cell cycle in phase G1 and the caspase-3 activity exhibited. The complex **3c** was the lowest number of caspase-activating cells (2.1%) compared with both the control and other complexes in MDA-MB-231 cells. But the complex **3a** was the highest number of

Abbreviation: Ag(I)-NHC, Silver (I)-N-Heterocyclic Carbene; ATCC, American Type Culture Collection; DMEM/F12, Dulbecco's Modified Eagle Medium/Nutrient Mixture F-12; DMSO, Dimethyl sulfoxide DNA, Deoxyribonucleic acid; MCF7, Human breast cancer cell line. (ATCC code: HTB-22TM); MCF 10A, immortalized breast cell line (ATCC code: CRL-10317TM); MEMM, Mammary Epithelial Basal Medium MDA-MB-231, Human breast adenocarcinoma cell line (ATCC code: HTB-26TM); MTS, [3-(4;5-dimethylthiazol-2-yl)-5-(3-carboxymethoxyphenyl)-2-(4-sulfophenyl)-2H-tetrazolium]; FBS, Fetal Bovine Serum FDA, Food Drug Administration; PBS, Phosphate Buffered Saline; WHO, World Health Organization; **3a**, Bromo-[1-(2-morpholinoethyl)-3-propylbenzimidazol-2-ylidene]silver(I); **3b**, Bromo [1-isopropyl-3-(2-morpholinoethyl)benzimidazol-2-ylidene]silver(I); **3c**, Bromo-[1-(3-hydroxypropyl)-3-(2-morpholinoethyl)benzimidazol-2-ylidene]silver(I).

* Corresponding author.

E-mail address: isil@beykent.edu.tr (I. Yıldırım).

<https://doi.org/10.1016/j.molstruc.2020.129462>

0022-2860/© 2020 Elsevier B.V. All rights reserved.

caspace-activating cells (% 9.6). These findings have shown that these new Ag(I)-NHC complexes can be important new anticancer agents for breast cancer treatments.

© 2020 Elsevier B.V. All rights reserved.

1. Introduction

Cancer is one of the most important health problems of our time. A report released in the 2019 year by the World Health Organization (WHO) [1] indicated that in 2018, it is estimated that 627,000 women died from breast cancer that is approximately 15 % of all cancer deaths among women. While breast cancer rates are higher among women in more developed regions, rates are increasing in nearly every region globally. U.S. Breast Cancer Statistics estimated [2]. 42,170 women in the U.S. are expected to die in 2020 from breast cancer. Death rates have been steady in women under 50 since 2007, but have continued to drop in women over 50. The overall death rate from breast cancer decreased by 1.3 % per year from 2013 to 2017. These decreases are thought to be the result of treatment advances and earlier detection through screening. Moreover, it was reported that breast cancer is the most common form of cancer in the United States. The National Cancer Institute (NCI) [3] estimated that the new cases in 2019 approximately 268,000 (15.2 %) women will be diagnosed with breast cancer for this year, and 41,760 (6.9 %) women will die of the cancer disease. The new drugs will inevitably be discovered to prevent or cure cancer with the justification that this rate of cancer growth and deaths will continue.

Cancer is a highly complex disease that associates with several processes including sustained proliferative signaling, unlimited replicative potential, and activation of invasion and metastasis. So, development of drugs or agents targeting any of these processes is important. Recently, there has been a growing demand for metal-based compounds in the treatment of cancer. Cisplatin and other platinum-based drugs are well-known valid anticancer drugs. However, during chemotherapy, the presence of numerous side effects and the onset of frequent phenomena of resistance have pushed many research groups to devise new metal-based compounds holding improved anticancer properties and fewer undesired effects. Amongst the variety of synthesized compounds, significant antiproliferative effects have been obtained by employing organometallic compounds, particularly those based on metal complexes. Recently, Ag(I)-NHCs have been developed the purpose of potential chemotherapeutic drugs as well. Several possible biological targets of Ag(I)-NHC complexes have been identified. However, the mechanisms of action of there are still unclear. Therefore, further research is required to fully elucidate the mechanism of action of these Ag(I)-NHC complexes.

Silver complexes are a good cytotoxic agent against many types of cancer cells as stated in current literature, and most of them exhibit lower toxicity than cisplatin. [4] Similarly, it identified that the cytotoxic properties of Ag(I)-NHC complex on MCF7 and MDA-MB-231 cell lines [5].

It reported that the cytotoxic effects of various Ag(I)-NHC complexes were carried out using MCF7 cells in different studies [6,7] and several possible biological targets of Ag(I)-NHC complexes have also been identified. The mechanism of action of silver cations is still not clear; however, it has been thought that silver cations bind to the cell surfaces and interact with the enzymes and proteins that are important for the cell wall synthesis [8–10]. Possibly this is the reason that the bonding of silver cations to biologically compatible ligands increase the bioavailability and ultimately the activity of silver cations as reported that previous study [11–13].

Although solubility and ionization of the metal sources are significant parameters to deal with metals in the biological system, lipophilicity, and low toxicity are the most important properties of cancer drugs. Functional groups including in NHC core have been shown to greatly affect the toxicity, with lipophilicity and counterion playing an important role. It has been established that lipophilic character depends on the chain length that eases the Ag(I)-NHC complexes to penetrate the cell membranes, where they release silver ions, which interact with cellular organelles and affect their functionalities [14,10,15]. The research on this subject is still ongoing. Although the cytotoxic activity of different Ag(I)-NHC complexes have become known recently times, the cytotoxic effects, lipophilic, and solubility properties of the benzimidazolium-functionalized Ag(I)-NHC complexes bearing 2-morpholinoethyl group have not examined as of yet. Therefore, we aimed to investigate the cytotoxic effect and apoptosis mechanism of new Ag(I)-NHC complexes on breast cancer cell lines (MCF7), breast adenocarcinoma cell lines (MDA-MB-231), and non-tumorigenic epithelium cell lines (MCF 10A). The new Ag(I)-NHC complexes were derived from morpholine-linked benzimidazole, synthesized, and determined in antimicrobial activity in our previous study.

2. Material method

2.1. Material

DMEM/F12 was purchased from Thermo Fischer Scientific. MEBM were purchased from Lonza. Apoptosis kits were purchased from BD (Becton, Dickinson and Company, USA), PBS, FBS, antibiotic (Penicillin-Streptomycin), Trypsin/EDTA solution and Cisplatin were purchased from Sigma-Aldrich (Germany). DMSO was purchased from Santacruz (Germany). MTS was purchased Promega (Germany).

2.2. Used devices

In this study, Nuve mark a laminar flow cabinet, Thermo Scientific mark a CO₂ Incubator, and an Emax[®] Plus Microplate reader was used.

2.3. Experimental

The chemicals used at work including 2-morpholino ethyl chloride, potassium hydroxide, 3-bromo-1-propanol, diethyl ether, dimethylformamide (DMF), etc. were purchased from Sigma-Aldrich, abcr and Merck. All other reagents were obtained commercially from Aldrich and used without further purification. Melting points were identified in glass capillaries under air with an Electrothermal-9200 melting point apparatus. On the other hand, FT-IR spectra assay were recorded in the range 400–4000cm⁻¹ on Perkin Elmer Spectrum 100 FTIR spectrometer. Carbon (¹³C) and Proton (¹H) NMR spectra were recorded using either a Bruker 400 Merkur spectrometer operating at 100 MHz (¹³C), 400 MHz (¹H) in CDCl₃ with tetramethylsilane as an internal reference. Elemental analyses were performed by Inonu University Scientific and Technology Centr (Malatya, TURKEY).

2.4. Synthesis of 1-(3-hydroxypropyl)-3-(2-morpholinoethyl)benzimidazolium chloride, 2

The reaction between 1-(3-hydroxypropyl)benzimidazole (1.05 g, 6 mmol) and 4-(2-chloroethyl)morpholine (0.90 g, 6 mmol) in acetonitrile (4 mL) gave compound 1. This mixture was stirred at 80 °C for 24 h. Then, the solvent was evaporated under vacuum to afford the product as a white solid. This solid was washed with diethyl ether (2 × 10 mL). The crude product was recrystallized from ethyl alcohol / diethyl ether (1:3) at room temperature to give white colored benzimidazolium salt [16]. Yield: 79% (1.54 g); m.p.: 211–212 °C; $\nu_{(\text{CN})}$: 1504 cm^{-1} . Anal. Calc. for $\text{C}_{16}\text{H}_{24}\text{ClN}_3\text{O}_2$: C: 58.98; H: 7.42; N: 12.90. Found: C: 58.05; H: 7.34; N: 12.96. ^1H NMR (400 MHz, CDCl_3) in δ ppm: 2.13 (s, 2H $-\text{CH}_2\text{CH}_2\text{CH}_2\text{OH}$); 2.58 (s, 4H $-\text{NCH}_2\text{CH}_2\text{O}-$); 2.94 (s, 2H $-\text{NCH}_2\text{CH}_2-\text{NC}_4\text{H}_8\text{O}$); 3.61 (s, 2H $-\text{NCH}_2\text{CH}_2-\text{NC}_4\text{H}_8\text{O}$); 3.61 (s, 2H $-\text{NCH}_2\text{CH}_2\text{CH}_2\text{OH}$); 4.74 (s, 4H $-\text{NCH}_2\text{CH}_2\text{O}-$); 5.13 (s, 1H $-\text{CH}_2\text{CH}_2\text{CH}_2\text{OH}$); 7.22–7.76 (m, 4H Ar-H); 10.96 (s, 1H 2-CH). ^{13}C NMR (100 MHz, CDCl_3) in δ ppm: 30.6 ($-\text{CH}_2\text{CH}_2\text{CH}_2\text{OH}$); 42.7 ($-\text{NCH}_2\text{CH}_2-\text{NC}_4\text{H}_8\text{O}$); 44.8 ($-\text{NCH}_2\text{CH}_2\text{O}-$); 52.8 ($-\text{NCH}_2\text{CH}_2-\text{NC}_4\text{H}_8\text{O}$); 55.2 ($-\text{NCH}_2\text{CH}_2\text{CH}_2\text{OH}$); 57.0 ($-\text{CH}_2\text{CH}_2\text{CH}_2\text{OH}$); 65.0 ($-\text{NCH}_2\text{CH}_2\text{O}-$); 113.1, 113.6, 127.3, 127.5, 127.6, 131.0, 131.2 and 131.3 (Ar-C); 143.5 (2-C)

2.5. X-ray crystallography

X-ray single-crystal diffraction data for the benzimidazolium salt 2 was collected at room temperature on a Rigaku-Oxford Xcalibur diffractometer with an EOS-CCD detector using graphite-monochromated MoK_α radiation $\lambda = 0.71073$ Å. Details of the data collection conditions and refinement processes are summarized in Table 1. Data reduction and analytical absorption correction was performed using CrysAlisPro 1.171.40.67a software [17]. The structure was solved with the ShelXT [18] solution program using dual methods and by using Olex2 [19] as the graphical interface. The

Table 1
Crystal data and structure refinement parameters for benzimidazolium salt 2.

CCDC number	2026786
Chemical formula	$\text{C}_{16}\text{H}_{24}\text{N}_3\text{O}_2\text{Cl}$
Formula weight (g/mol)	325.83
Temperature (K)	295
Crystal system	Orthorhombic
Space group, Z	$Pbca$, 8
Crystal size (mm^3)	$0.45 \times 0.32 \times 0.23$
Crystal shape/color	block, colourless
a (Å)	12.0113(13)
b (Å)	13.5396(10)
c (Å)	21.258(2)
α, β, γ (°)	90
Volume (Å ³)	3457.1(6)
$T_{\text{min}}, T_{\text{max}}$	0.949, 0.962
$F(000)$	1392
Abs. Coeff. μ (mm^{-1})	0.232
Calc. Density (g cm^{-3})	1.252
θ range (°)	3.158–25.021
$h_{\text{min}}, h_{\text{max}}$	–13, 14
$k_{\text{min}}, k_{\text{max}}$	–16, 10
$l_{\text{min}}, l_{\text{max}}$	–25, 15
Measured refls	6989
Independent refls	3042
Observed refls	1537
Parameters, restraints	203, 0
R_{int}	0.0549
Goodness of Fit on F^2	0.997
R indices [$I > 2\sigma(I)$]	$R_1 = 0.0589, wR_2 = 0.1018$
$\rho_{\text{max}}, \rho_{\text{min}}$ ($\text{e} \text{Å}^{-3}$)	0.182, –0.260
$(\Delta/\sigma)_{\text{max}}$	<0.0001

model was refined with ShelXL 2018/3 [20] using full matrix least squares minimization on F^2 . All non-hydrogen atoms were refined an isotropically. All H atoms except for H1 were positioned geometrically and refined using a riding model, fixing the aromatic C–H lengths at 0.93 Å, methylene C–H lengths at 0.97 Å. H1 atom involved in hydrogen bond was found in the difference map and refined freely.

2.6. Cell line

MCF7, MDA-MB-231 and MCF 10A were obtained from ATCC.

2.7. Cells culture and treatment

MCF7 and MDA-MB-231 cells were grown in a DMEM: F12 medium, MCF 10A cells were grown in MEBM at a temperature of 37 °C in a humidified incubator with a 5 % CO_2 atmosphere. The test matters were dissolved in dimethyl sulfoxide (DMSO) in a stock solution, and then it was diluted to the required concentrations. A total of 70–80 % confluent cells were treated with concentrations from 1 μM to 100 μM in all test matters for 24 and 72 h in the growth medium.

2.8. Cell proliferation assay with MTS

The MTS assay is a colorimetric assay for assessing a cell's metabolic activity. The MTS tetrazolium compound is bio-reduced by cells into a colored formazan product that is soluble in the culture medium. This conversion is presumably accomplished by NADPH or NADH produced by dehydrogenase enzymes in metabolically active cells [21].

Measurement of the anti-proliferative effect using the MTS cell proliferation kit was performed in a 96-well plate using human breast cell lines. Cells were grown in the appropriate medium and then seeded in 96 well plates in a 10 μL medium. The presence of 1500 cells in each well was verified and then incubated at 37 °C in a 5% CO_2 atmosphere for 24 h. At the end of the time cycle, different concentrations from 1 to 100 μM of the test sample were added. The cells were then incubated under conditions appropriate for the cell lines ranging from 24 to 72 h. Concentration was adjusted from 1 μM to 30 μM both hours. Then, 5 μL of MTS reagent was added to each well and incubated for 1 h. At the end of the incubation time, the optical density (OD) of the color was measured using a microplate reader. It found a primary wavelength of 490 nm. The mean absorbance values were calculated and the cell viability percentages were documented using the Excel Office program. Then the IC_{50} values were calculated. The results are shown in Table 2. Apoptosis studies were performed according to the determined IC_{50} values.

2.9. Apoptosis detection by staining with Annexin V-FITC and propidium iodide (PI)

Annexin V-PI FITC apoptosis detection kits were used to detect the apoptosis method [22] as described by the manufacturer. All cells were seeded in a 6-well plate with 2×10^5 cells/mL and incubated for 24 h. At the end of the incubation period, test substances with known IC_{50} values were added and then allowed to incubate for another 24 h. The samples were placed in a centrifuge and the supernatant was discarded. The cells were washed twice with cold PBS (2 mL), and then the cells were re-suspended in 1 mL 1X Binding Buffer solution. The solution was then transferred through the flow tube. Then the cells were re-suspended in 100 μL 1X Binding Buffer solution. Then 5 μL of Annexin V and 5 μL of PI were added. The cells were gently mixed and incubated for 20 min in the dark. 400 μL of 1X Binding Buffer was added to each tube.

Table 2
Cytotoxicity effects against MCF7, MDA-MB-231 and MCF 10A cells.

Compound	IC ₅₀ Values μ M				
	24 h			72 h	
	MCF7	MDA-MB-231	MCF 10A	MCF7	MCF 10A
3a	18 \pm 2.12	8	18 \pm 2.82	8 \pm 6.73	14 \pm 0.0
3b	17 \pm 1.41	7.5 \pm 0.77	14 \pm 2.72	7.5 \pm 2.51	15.5 \pm 1.41
3c	23 \pm 7.63	12 \pm 1.69	25 \pm 1.14	5 \pm 2.54	25 \pm 4.87
Cisplatin	>50	27 \pm 4.90	28 \pm 6.63	>50	1–100 μ M NI

NI: No inhibition; \pm have shown SD. There no found \pm SD values for **3a** complex in MDA-MB-231.

The samples were then analyzed by flow cytometry within 1 h. At least 10,000 cells were analyzed per sample [23].

2.10. Cell cycle analysis

Measuring the DNA content of cells was performed on a BD flow cytometer and using the BD Cycle test™ Plus DNA reagent [24]. Breast cells were seeded on the 6-well plate with 2×10^5 cells/mL and incubated for 24 h. At the end of the incubation period, test substances with known IC₅₀ values were added and allowed to incubate for 24 h. Cells were harvested from the plate into 50 mL conical tubes and centrifuged 5 min. The supernatant was removed. 50 μ L of PBS was added onto the pellet and suspended. The pellet was transferred to the flow tube. The cell pellets were washed twice with 1 mL of the buffer solution provided by the manufacture. The pellet was then centrifuged at a low rpm for 5 min. After removal of the supernatant, the remaining pellet was resuspended again with 1 mL of BD buffer solution. The cell suspension was incubated in the dark at room temperature and was analyzed by the BD flow cytometry.

2.11. Apoptosis detection by caspase-3 activation

Measurement of the caspase-3 active-cells was performed on a BD flow cytometer and using a BD FITC Active Caspaz-3 Apoptosis kit [25]. Breast cells were seeded into a 6-well plate with 2×10^5 cells/mL and incubated for 24 h. At the end of the incubation period, test substances with known IC₅₀ values were added and allowed to incubate for 24 h. Cells were harvested from the plate into 50 mL conical tubes and centrifuged for 5 min. The supernatant was removed. Then the pellet cells were washed twice with cold 1X PBS solution. Then the pellet cells were re-suspended in 500 μ L of BD Cytofix/Cytoperm™ solution for permeabilized. Incubated cells for 20 min on ice and then centrifuged for 5 min discarding the BD Cytofix/Cytoperm™ solution. The samples were then washed twice with a 500 μ L BD Perm/Wash™ buffer (1X). Cells were then incubated with 20 μ L of cleaved caspase-3 (Asp 175) BD rabbit polyclonal antibody and incubated for 30 min at room temperature. Then the pellet was re-suspended again in 1 mL of BD buffer solution and then re-suspended in 0.5 mL BD Perm/Wash™ buffer (1X) and then transferred to the flow tube and analyzed by flow cytometry. At least 10,000 cells were analyzed per sample [23].

2.12. Statistical analysis

Statistical analysis for cytotoxicity was performed by using the Excel software program and a comparison between mean values for cytotoxicity was calculated by Student's *t*-tests. Analysis of variance and difference was considered significant at $p < 0.05$, $p < 0.001$, and $p < 0.001$.

3. Results

3.1. Synthesis

Before this study, we synthesized the salt of "1-(3-hydroxypropyl)-3-(2-morpholinoethyl) benzimidazolium bromide" and their Ag(I)-NHC complexes **3a-c** [16]. We could not determine any cytotoxic, antiproliferative, or cytostatic effects of the benzimidazolium salt we synthesized on breast cancer cells. So, we worked again to determine the effects of salt on cancer cells by replacing the halogen in the salt (using chlorine instead of bromine atoms), and synthesized the 1-(3-hydroxypropyl)-3-(2-morpholinoethyl) benzimidazolium chloride salt **2** (Scheme 1). But we could not determine any cytotoxic, antiproliferative or cytostatic effects of the benzimidazolium salt we synthesized on breast cancer cells and we took into consideration the silver compounds associated with the ligands we synthesized earlier. Because a very low cytostatic activity could be seen in the previous ligands at a concentration $p > 500 \mu$ M.

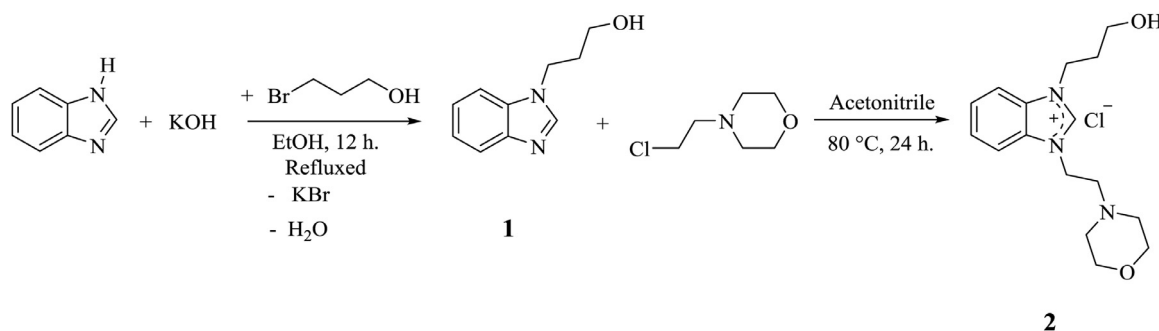
For the synthesis of the new morpholinoethyl substituted benzimidazolium salt **2** in this study; firstly, we obtained 1-(3-hydroxypropyl)benzimidazole from the reaction of benzimidazole and 3-bromopropanol. Then, from the reaction of 1-(3-hydroxypropyl)benzimidazole and 4-(2-chloroethyl)morpholine were obtained the 1-(3-hydroxypropyl)-3-(2-morpholinoethyl) benzimidazolium chloride **2** (Scheme 2). The new benzimidazolium salt **2** was obtained as a white solid in 79 % (1.54 g) yield. The ¹H NMR of benzimidazolium salt in CDCl₃ displayed the -OH proton at 5.13 ppm and the characteristic 2-CH proton at 10.96 ppm. In the ¹³C NMR, the characteristic 2-C signal appeared at 143.5 ppm for benzimidazolium salt **2**. Other ¹H NMR and ¹³C NMR peaks (Fig. S11) are compatible with similar bromine salt [16]. FT-IR spectrum of the benzimidazolium salt **2** showed a band at 1504 cm⁻¹ corresponding to the vibrations of C=N of the benzimidazolium salt [16]. The result of the elemental analysis demonstrates that the calculated value for benzimidazolium salt was very close to the found value (Scheme 2).

3.2. Cytotoxicity effect results

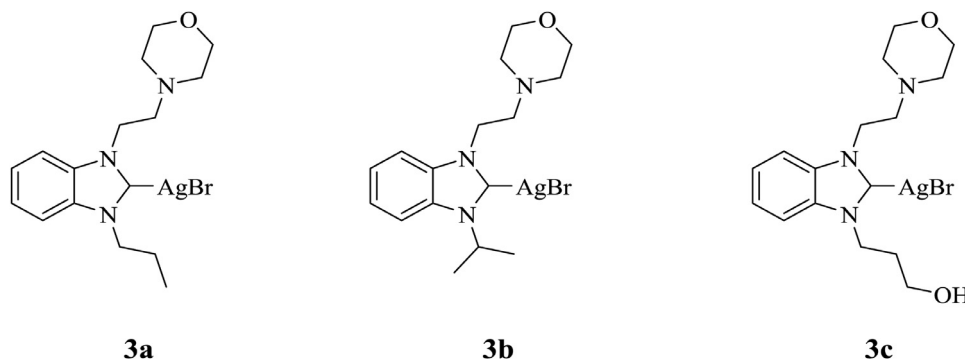
Cytotoxicity assays for **3a**, **3b**, **3c** and cisplatin were carried out in all cell types, IC₅₀ values were calculated for only the silver complexes **3a-c** and apoptotic mechanism studies continued with IC₅₀ of these complexes.

IC₅₀ values of **3a-c** complexes and cisplatin are given in Table 2. Considering in the Table 2, **3a** complex with the 3-propyl substituent was more cytotoxic in MCF7 cells than compared with the non-tumorigenic epithelial cell line, (MCF 10A) after 72 h of incubation. The **3a** complex was less cytotoxic in MCF7 cells compared with the MDA-MB-231 adenocarcinoma cells after 24-hours of incubation.

The **3b** complex with the 3-isopropyl substituent was more cytotoxic in MDA-MB-231 cells compared with both MCF7 and MCF 10A cells after 24 h of incubation. The **3b** complex was more cyto-



Scheme 1. Synthesis of 2-morpholinoethyl-substituted benzimidazolium Salt **2**.



Scheme 2. Structure of 2-morpholinoethyl substituted Ag(I)-NHC complexes **3a-c** [16].

toxic effect than cisplatin, complex **3a**, and complex **3c** in MDA-MB-231 cells compared with both MCF7 and MCF 10A cells after 24-hours of incubation. In regards to the 72-hour results, in the MCF7 cells, complex **3b** was more cytotoxic compared with the **3a** complex, while it showed less cytotoxic effect than complex **3c**. Compared with MCF 10A cells, complex **3b** complex showed a stronger cytotoxic effect than the MCF 10A cells after 72 h incubation.

After 24 h' incubation, the 3-hydroxypropyl-substituted compound, complex **3c** had relatively weak cytotoxic effects compared with other compounds including cisplatin, with IC_{50} values of 23, 12, and 25 μ M in MCF7, MDA-MB-231, and MCF 10A cells, respectively.

Complex **3c** was more cytotoxic than cisplatin, complex **3a**, and complex **3b** in MCF7 cells compared with the MCF 10A cells after 72 h of incubation. Complex **3c** was more cytotoxic in MCF7 cells than in MCF 10A cells after both 24 and 72 h of incubation.

Fig. 1 shows that the compounds decreased cell proliferation in a dose-dependent manner in MCF7, and MCF 10A cells after 24 and 72 h of incubation period and in MDA-MB-231 cells after a 24 of hour incubation period.

When MCF7 cells were incubated with complex **3a** for 24 h, there was no significant difference in cell viability of 2.5, 5, and 10 μ M concentrations, but the 15; 20; and 30 μ M concentrations were found significantly different in cell viability $p < 0.05$; $p < 0.01$; and $p < 0.001$ levels, respectively. The complex **3a** exhibited a significant difference $p < 0.05$ level at a concentration of 5 μ M. Moreover, in 10; 15; 20, and 30 μ M concentrations were significant difference at the $p < 0.001$ level when compared with the control group after 72 hours' incubation.

When MDA-MB-231 cells incubated with complex **3a** complex for 24 h, it showed a significant difference $p < 0.05$ at a concentration of 10 μ M at a level of, whereas it showed significant differences $p < 0.01$ at 5; 15; 20; and 30 μ M concentrations compared with the control group.

When MCF 10A cells were exposed to the **3a** complex at 24 h then compared with the control group at a concentration of 20 μ M and 30 μ M, it showed a significant difference $p < 0.05$; $p < 0.001$ respectively. **3a** complex for 72 h compared with the control group, a significant difference was found 15; 20, and 30 μ M concentrations ($p < 0.05$).

When MCF7 cells incubated with **3b** complex for 24 h no significant difference in was observed concentrations of 7.5 and 10 μ M compared with the control group, but 12 μ M ($p < 0.01$), and concentration of 20 and 30 μ M caused a significant difference as a $p < 0.001$. A 72-hour incubation with complex **3b** was compared with the control group at a concentration of 7.5 μ M ($p < 0.01$), while concentrations of 10; 12; 16; 20; and 30 μ M showed a significant difference at $p < 0.001$ level.

When MDA-MB-231 cells incubation with **3b** complex for 24 h, showed a significant difference $p < 0.05$ levels at a concentration of 10 μ M and 30 μ M, but in concentration of 16 and 20 μ M $p < 0.01$ compared with the control groups.

When MCF 10A cells incubated with complex **3b** for 24 h, a significant difference was observed at a concentration of 16 and 20 μ M $p < 0.01$ and at 30 μ M concentrations $p < 0.05$ level compared with the control group. When complex **3b** complex incubated for 72 h in the concentration of 16 μ M showed significant difference $p < 0.01$ and in 20 and 30 μ M concentrations $p < 0.001$ level compared to the control group.

When the MCF7 cells incubated with **3c** complex for 24 h, a significant difference was observed at concentration of 14; 20; 30 μ M when compared with the control group ($p < 0.05$, $p < 0.01$ $p < 0.001$ levels, respectively). Incubation of MCF7 cells with complex **3c** for 72 h at a concentration of 4 μ M, it exhibited a significant difference $p < 0.05$ level, while the concentrations of 10 and 14 μ M $p < 0.01$ level; 6; 20; and 30 μ M concentrations had significant difference at $p < 0.001$ level exhibited.

When MDA-MB-231 cells were exposed to complex **3c** for 24 h at a concentration of 14 μ M, a significant difference was observed

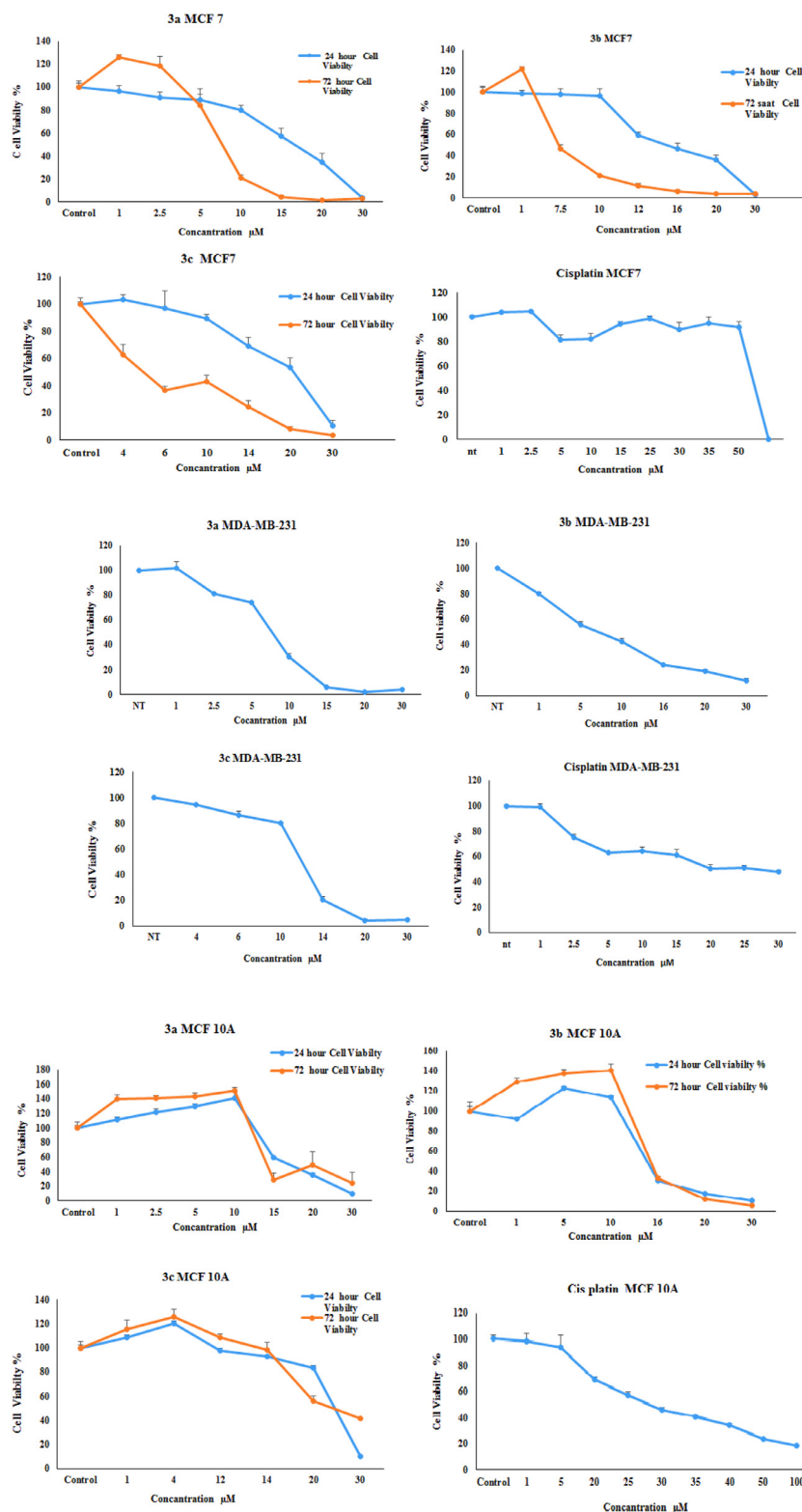


Fig. 1. Cytotoxic activity of **3a**, **3b**, **3c** and cisplatin on MCF7, MCF 10A cell after 24, and 72 h of the incubation period. But cytotoxic activity of **3a**, **3b**, **3c** and cisplatin on MDA-MB-231 was 24 h. Values are represented as mean \pm SD ($n = 4$).

when compared with control ($p < 0.05$). A significant difference was also observed at concentrations of 20 μM ($p < 0.01$) and 30 μM ($p < 0.001$).

When MCF 10A cells were incubated with complex showed **3c** for 24 h at concentrations of 14 and 30 μM , a significant difference at the level of $p < 0.001$ at 30 μM concentration was observed

when compared to the with the control group. ($p < 0.01$). A significant difference was also observed at a concentration of 20 μM ($p < 0.05$). A 72 -h incubation with 30 μM of complex **3c** showed a significant difference compared with control ($p < 0.001$).

MCF7 cells incubated with cisplatin for 24 h showed a significant difference ($p < 0.01$) at a concentration of 10 μM compared

with the control group. Cisplatin showed significant differences in MDA-MB-231 cells at concentrations of 5 and 30 μM ($p < 0.01$ levels) and at 20 and 25 concentrations of 20 and 25 μM ($p < 0.05$) compared to with control group. Cisplatin for a 24 -h incubation with cisplatin had no significant effect at 1 and 5 μM concentration, but a significant difference was observed at a concentration of 20 μM , ($p < 0.05$;) and at concentrations of 25; 30; 35 and 40, and 100 μM concentrations ($p < 0.01$), and 50 and 100 μM ($p < 0.001$) in MCF 10A cells.

3.3. Apoptosis mechanisms

3.3.1. Determination of apoptotic activity by Annexin V-P1

Annexin A5 (or annexin V) is a cellular protein in the Annexin group. In flow cytometry, Annexin V is commonly used to detect apoptotic cells by its ability to bind to phosphatidylserine, a marker of apoptosis when it is on the outer leaflet of the plasma membrane. Apoptotic cell death was determined by using the Annexin V method.

Compared with both control and other complexes, complex **3a** achieved the earliest apoptotic cell death when compared with other cancer cell lines and the non-tumorigenic epithelial cell line (MCF 10A). showed that complex **3a** was the highest early apoptotic cell with a value of 8.1 % in MCF 10A cells. When the total number of apoptotic cells (early [Q4] + late [Q2]) was considered, complex **3a** caused the highest degree of apoptotic cell death deaths of all the cells.

Complex **3b** caused total apoptotic cell death in both MCF 10A and MDA-MB-231 cells. It showed an early apoptotic cell death of 1.9 % in MCF7 cells. When the total number of apoptotic cells (early [Q4] + late [Q2]) was considered, complex **3b** caused the higher apoptotic cell death in MDA-MB-231 cells than MCF7 cells.

Complex **3c** complex caused early apoptotic cell death by the second cycle with a value of 7.1 % in MDA-MB-231 cells. In addition, complex **3c** caused early apoptotic cell death by the second cycle with a value of 4.9 % in MCF 10A cells.

3.3.2. Cell cycle analysis results

The induction of cell death along with cell-cycle arrest is one of the foremost mechanisms regulating cell growth. In the human breast carcinoma cell lines, we investigated these agents for the relative contribution of these mechanisms to growth inhibition in culture. The MCF7 cell population in G1 and S phase presence of the complex **3a** increased by 3.2 % and 3.4 %, respectively, when compared with control. An increased cell population in phase S indicates that cells-maintained DNA replication.

According to Fig. 3, the population of MCF 10A cells in the G1 phase in presence of complex **3a** increased to 5.4 % compared with control group, while the population of cells in the G2 and S phases decreased to 0.4 % and 0.5 %, respectively. This indicates that complex **3a** damages DNA in MCF 10A cells and that these cells are in the G1 / G0 phase.

The cell population for **3a** complex decreased by 11.8 % when compared with the control at the G1 phase in the MDA-MB-231 cancer cells. Although the cell population of MCF 10A cells in the G1 phase, the population of cells decreased in MDA-MB-231 cells. The tested have inhibitory effects on cancer cell DNA.

Although the population increased slightly in the presence of **3b** complex compared with the control point during the G1 and S phases, the population of cells at the G2 / M control point was reduced by 15.2 % compared to the control group of MCF7 cells. The population of MDA-MB-231 cells for complex **3b** decreased by 11.8 % compared to control at the G1 phase.

The population of MCF7 cells in the G1 phase increased by 6.2 % in the presence of complex **3c** compared with control. The MDA-MB-231 cell count in the G1 phase was further reduced to

Table 3

Selected bond lengths Å, bond and torsion angles ($^{\circ}$) and hydrogen bond geometry.

Bond lengths			
C1–N1	1.327(4)	C1–N2	1.327(4)
N1–C2	1.388(4)	N2–C7	1.390(4)
C2–C7	1.379(4)	N1–C14	1.469(4)
N2–C8	1.467(4)	O1–C16	1.382(4)
Bond and torsion angles			
N1–C1–N2	110.3(3)	C1–N1–C2	108.3(3)
C1–N2–C7	108.0(3)	C1–N1–C14	124.7(3)
C1–N2–C8	124.5(3)	C1–N2–C8–C9	78.2(4)
N2–C8–C9–N3	–60.1(4)	C1–N1–C14–C15	–104.0(4)
O1–H1...C11 hydrogen bond geometry			
O1–H1	H1...C11	O1...C11	O1–H1...C11
0.86(4) Å	2.22(4) Å	3.081(3) Å	178(4) $^{\circ}$

27 % compared with control. The population of MCF 10A cells in the presence of complex **3c** was reduced in all cell-cycle phases (Figs. 2.1, 3.1, 3.2 and 4.1).

Considering all the results, show that the effects of the tested compounds in cancer cells are greater than effective than all control points in the non-tumorigenic epithelial cell line (MCF 10A). The fact that population of cells shows that does is less damaging to the non-tumorigenic epithelial cell line (MCF10A).

3.3.3. Determination of caspase-3 activity

Compounds **3a-c** had caspase-3 activating effects in both MCF 10A cells and MDA-MB-231 cells. The findings show that these compounds stimulate apoptosis by increasing caspase-3 activity to a certain degree at the determined IC_{50} values.

According to Fig. 4, complex **3a** had the same effect as a control in MCF 10A cell. It was the highest number of caspase-activating cells (9.6 %) compared with both control and other complexes in MDA-MB-231 cells. According to the results given in Fig. 4, the **3b** complex showed a similar effect in both cancer cells and non-tumorigenic epithelial cell line (MCF 10A).

3.3.3.1. Crystal and molecular structure of benzimidazolium salt 2.

X-ray single-crystal diffraction analysis reveals that the molecular structure of the benzimidazolium salt **2** has a cation molecule consisting of hydroxypropyl and morpholinoethyl attached N-benzimidazole ring and a chloride anion linked to the cation through a hydrogen bond (Fig. 5). Selected bond lengths, bond, and torsion angles including geometrical details of H-bond are given in Table 3. The N-benzimidazole ring is planar with a maximum deviation of 0.024(3) Å for C7 atom. C1–N bond lengths of 1.327(4) Å, and the other C–N bond lengths in benzimidazole ring agree well with those of a similar structure in literature {1.325(4) Å and 1.328(4) Å for C1–N, 1.386(3) Å and 1.386(4) Å for the other C–N lengths [26]}.

The morpholine ring in the benzimidazolium salt **2** adopts a chair conformation, with a total puckering amplitude of $Q_T = 0.901(1)$ Å. The plane through the C atoms of the morpholine ring makes a dihedral angle of 67.63(10) $^{\circ}$ with the mean plane of benzimidazole ring. In the absence of intermolecular hydrogen bonds, the crystal structure of the benzimidazolium salt **2** is stabilized by weak intermolecular interactions. Crystal packing diagram of the benzimidazolium salt **2** can be found in supplementary information (Fig. SI2).

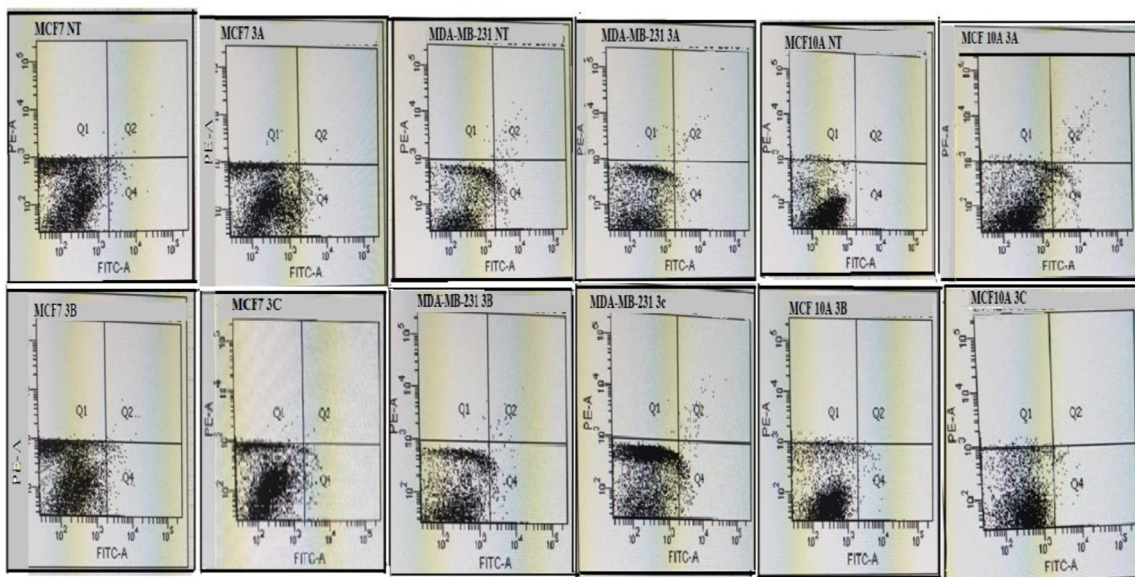
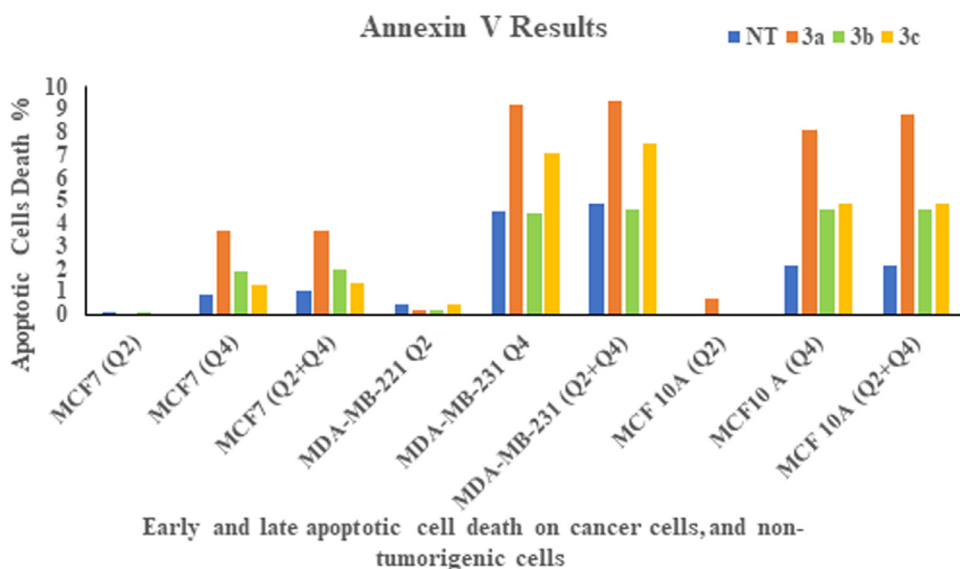


Fig. 2.1. Apoptotic effect of **3a**, **3b**, **3c** complexes on the MCF7, MDA-MB-231 and MCF 10A cells after 24 h of incubation period for IC₅₀ values. NT: Non treatment(or Control groups) Q1: necrotic cell, Q2: late apoptosis; Q3: live cell; Q4: early apoptotic cells.



Early and late apoptotic cell death on cancer cells, and non-tumorigenic cells

Fig. 2.2. **3a**, **3b**, **3c** Annexin V-PI analysis result on the MCF7, MDA-MB-231 and MCF 10A cells at 24 h for IC₅₀ values. NT: Non treatment(or Control groups) Q2: late apoptosis; Q4: early apoptotic cells.

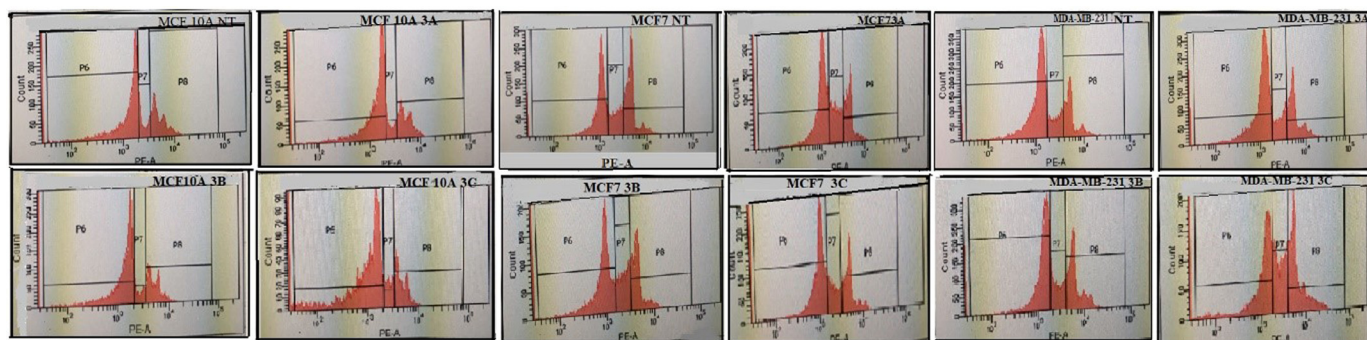


Fig. 3.1. Cell Cycle analysis histogram data NT: Non-treatment groups (or Control groups); **3a**, **3b**, **3c** complexes on the MCF7, MDA-MB-231 and MCF 10A cells after 24 h of incubation period for IC₅₀ values.

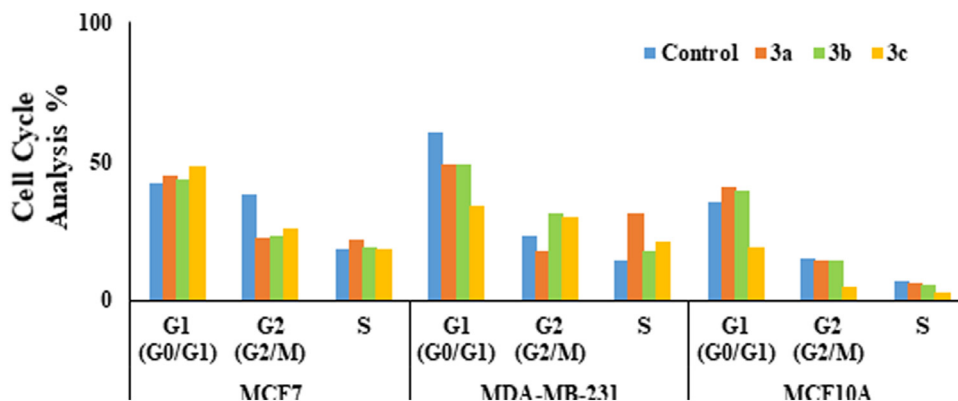


Fig. 3.2. **3a, 3b, 3c** Cycle analysis result on the MCF7, MDA-MB-231 and MCF 10A cells at 24 h for IC₅₀ values.

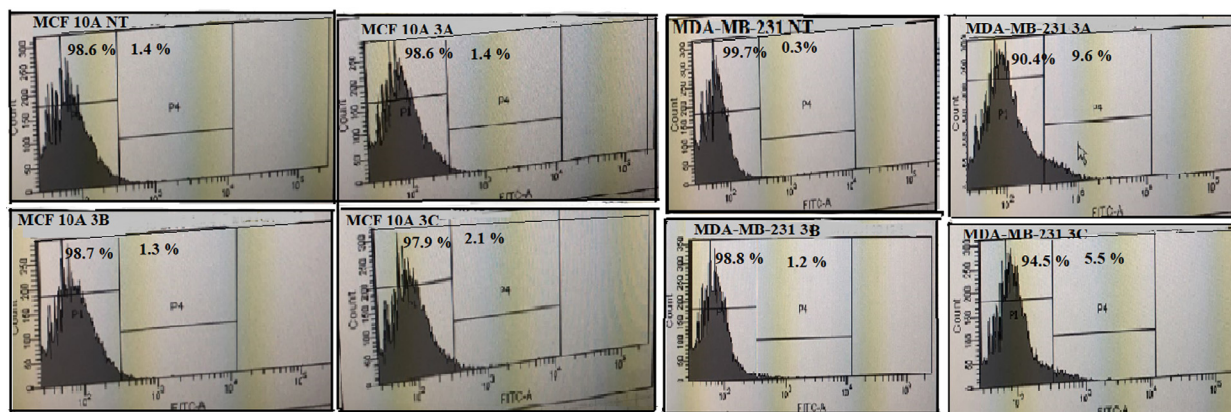


Fig. 4.1. **3a, 3b, 3c** Caspase analysis result on the MCF7, MDA-MB-231 and MCF 10A cells at 24 h for IC₅₀ values.

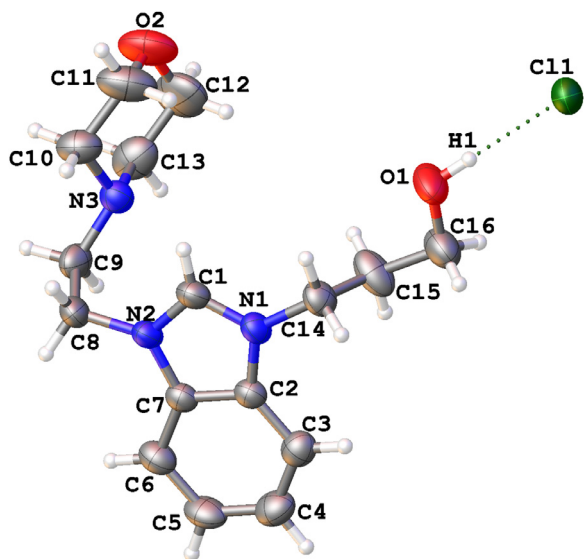


Fig. 5. The asymmetric unit of the benzimidazolium salt **2** showing the atom-labeling scheme. Anisotropic displacement ellipsoids are drawn at the 50% probability level.

4. Discussion

To synthesize NHCs, the more common practice is substitutions of alkyl/aryl groups at the nitrogen of azoles (imidazole, benzimidazole, triazole, etc.) to synthesize azolium. There are numerous ways to generate free NHCs and their metal complexes. The vari-

ability of the anticancer activity of NHC complexes highly depends on ring size and substituents. In this study, Ag(I)-NHC complexes **3a-c** of the n-propyl, isopropyl and 3-hydroxypropyl substituent depend on benzimidazole core were used since to be thought to have low toxicity. It is also important to note that the n-propyl substituent at position-1, and isopropyl group at position-1 are important for anticancer activity compared to 3-hydroxypropyl. Because these groups are lipophilic, whereas the 3-hydroxypropyl group is high water solubility and hydrophilic properties. The presence of CH₂, and electrostatic interactions, facilitate the activity of complexes, but O–H, which responsible for the H bond, increases polarity. This situation has been seen in the X-ray crystal structure.

In this study, MCF7 and MDA-MB-231 breast carcinoma cells were preferred selective targets and non-tumorigenic epithelial cell line, (MCF 10A) was used to determine nontoxic effects. The IC₅₀ values showed that cisplatin reduces cell growth at very high concentrations in cancer cells. Intake care of Table 2 results, **3a, 3b, 3c** complexes with 20 μM concentration, closest to the IC₅₀ value of all compounds were found significantly different $p < 0.05$; $p < 0.001$; and $p < 0.01$ in MCF7 cells. However, **3a, 3b, 3c** complexes with 10 μM concentration, closest to the IC₅₀ value of all compounds were found significantly different $p < 0.05$; $p < 0.01$; and $p < 0.001$ in MDA-MB-231 cells. Compared with the cytotoxic activity Ag(I)-NHC complexes, although the benzimidazole core was identical, the cytotoxic effects varied due to the difference substituents on the benzimidazole core.

When Ag(I)-NHC complexes **3a-c** were compared with cisplatin, they were three-fold more active in MCF7 cells after 24 and 72 h of incubations. Silver complexes **3a-c** were more cytotoxic than cisplatin in MCF7, MDA-MB-23, MCF 10A cells. This cytotoxic effect is likely due to the lipophilic nature of silver complexes, which aids

the transport of silver cations into the cell and subsequently into organelles where silver may contribute to toxicity by inhibiting cellular respiration and biomolecule metabolism.

Liu and co-workers [27] performed the results of a cytotoxicity study on a series of silver carbene complexes in MCF7 cells after 72 h of incubation. The IC_{50} values were range from 3.5 to 9.2 μM , while IC_{50} of cisplatin was 1.6 μM after 72 h of incubation. The values in our study (Table 2) are similar to the study of Liu and co-workers. Also, Silver compounds **3a-c** was more cytotoxic effect in MCF7 compared with the MCF 10A after 72 hours' incubation.

A study published in the 2016 year, showed that the IC_{50} value of benzimidazole-derived Ag(I)-NHC complex after 24 hours' incubation on MDA-MB-231 cells was 11.98 μM after 24 hours' incubation. In this study, complex **3c** was less cytotoxic activity, while complexes **3a**, **3b** more cytotoxic activity, which is the contrast to the results of a previous study [28]. The present also investigated the anti-proliferative activity of a series of Ag(I)-NHC complexes and Tamoxifen in MCF7 cells after 24 h of incubation [29]. In this study, complex **3c** was lesser cytotoxic activity than previous studies, but complexes **3a**, **3b** was parallel to the previous study (Table 1).

Another study, it was determined that the cytotoxic effect of bis-NHC coordinated silver(I), and it was found that Ag(I)-NHC complexes were exhibited a cytotoxic effect 1–5 μM concentration in the both MCF7 and MDA-MB-231 cells at 24, 48, and 72 h. Moreover, these complexes were exhibited a high cytotoxic effect compared to L929 normal cells. Considering these results more effective than our results. This statue may be associate with the alkyl chain length [30].

The complex **3b** exhibits the most cytotoxic activity compared to other complexes and cisplatin after incubation of 24 h. When the complexes are compared with each other, the **3a** and **3b** complex showed parallel activity, while the **3b** complex showed 1.5 times better cytotoxic activity than **3c**. Moreover, MDA-MB-231 cells were examined after a 72 -h incubation period and, while strong inhibition was only observed with concentrations of 20–30 μM . But the cytotoxic effect was not observed at other concentrations.

A cell cycle is a series of events that take place in a cell as it grows and divides. A cell spends most of its time in what is called interphase, and during this time it grows, replicates its chromosomes, and prepares for cell division. The cell then leaves interphase, undergoes mitosis, and completes its division. In the human breast carcinoma cell lines, we investigated these agents for the relative contribution of these mechanisms to growth inhibition in culture. We determined that Ag(I)-NHC complexes induced by apoptosis was associated with stopping the cell cycle in phase G1. Previously study it was found that especially with cis-platin-treated MCF7 cells, was the formation of numerous micronuclei (in up to 30 % of the cells) and an increase in the number of binucleate cells (up to 20%) [31].

In this study, apoptosis only MDA-MB-231 cells were analyzed due to caspase-3 deletion in MCF7 cells [32]. Fig. 1 shows that for the complexes; decreased cell proliferation in a dose-dependent manner in MDA-MB-231 cells after 24h incubation. According to the results given Fig. 4, the **3c** complex showed lesser effective caspase activation than the control group and other complexes **3a**, **3b** with a value of 2.1 % in MCF 10A cells. According to the results given in Fig. 4, the **3c** complex showed mo. In addition, it had the second-highest number of caspase-activating cells with 9.6 % compared to both control and other complexes in the MDA-MB-231 cell. As a result, the apoptotic effect of Ag(I)-NHC complexes in MDA-MB-231 cells has been determined, and treatment with all compounds caused cancer-cell death via the intrinsic apoptotic pathway. Tre lesser effective caspase activation than the control group and other complexes **3a**, **3b** with a value of

2.1% in MCF 10A cells. This effect is thought to be effective in other cellular apoptotic mechanisms, such as mitochondria disruption, cytochrome c release in cancer-cell cytoplasm, and the intracellular production of reactive oxygen species, as well as caspase-3 activation. Also, it may be thought of targeting Bcl-2 proteins by small molecules or activating alternative pathways to bypass Bcl-2-mediated protection to promote apoptosis. Previously a study, it was reported that cisplatin treatment overcomes Bcl-2-mediated protection in MCF7 cells (wt. p53), but not in MDA-MB-231 cells (mt p53), whereas a Taxane (paclitaxel) or a small-molecule Bcl-2 inhibitor (HA14-1) failed to act similarly. They also find that p53-dependent Noxa upregulation and lipid peroxidation associate with this process [33]. The incubation of cells with Ag(I)-NHC complexes in the presence of inhibitor may help to determine the mechanisms by which apoptotic cell death. In another study reported that the pro-apoptotic mechanism of action of unsymmetrically substituted benzimidazolium-functionalized Ag(I)-NHC compounds using Rhodamine 123 test and found that the tested compound induces apoptosis via the extrinsic mitochondrial pathway [34]. The literature and our study demonstrate Ag(I)-NHC complexes induce apoptosis by both intrinsic and extrinsic pathways. Supporting studies will further validate the importance of the findings of this study, and it is thought that it will allow the Ag compounds to be used as anticancer drugs.

5. Conclusion

Consequently, we have reported the synthesis of a new benzimidazolium salt bearing morpholino ethyl group. The new benzimidazolium salt has been characterized by using 1H NMR, ^{13}C NMR, FTIR spectroscopy, and elemental analysis technique. The molecular structure of this compound was confirmed by the X-ray diffraction method. The Ag(I)-NHC complexes **3a-c** have been identified as exhibiting anti-proliferative activity on the MCF7, MDA-MB-231 breast cancer cells. Considering all the time found that these silver compounds were found to be more active compared with cisplatin for 24- and 72 -h' incubation. These compounds may be suggesting an alternative agent to the cisplatin. All Ag(I)-NHC complexes **3a-c** were the most effective compounds. Biological activity depends on the nature of the group bound to benzimidazole and cancer cell line.

Apoptosis assays were carried out with all these compounds and had various degrees of stimulations on the apoptosis in each cell lines. Although our study is limited, mitochondrial membrane potential analysis, analysis of genes (Bax, Bcl-2 and caspase-3 and others such as the activity of caspase-8, caspase-9) that may be related to PCR, and protein expression levels by the western blotting needs to be done. A more detailed investigation of the study of the molecular mechanisms of these complexes will allow the identification of new targets for breast cancer treatment. So, we may be the future planned objectives of the study. We can predict what the next period will bring with new studies that will directly affect us and offer opportunities. One of these mechanisms may be the thioredoxin (Trx) system which is central in upholding the thiol redox homeostasis within the cell. Also, the thioredoxin system is involved in a wide range of biological functions within the cell, including ROS scavenging, DNA synthesis, cell proliferation, apoptosis, and cell signaling. Moreover, high expression rates of Trx and TrxR in cancer cells may be directly related to difficult-to-treat carcinomas of the breast. Recognizing the biological processes underlying in the disease, and the associated with molecular mechanisms in the various treatments that all play an important role in the development of anti-cancer drugs which can be used to prevent or inhibit the growth of cancerous cells.

Declaration of Competing Interest

The authors declare that they have no known competing financial interests or personal relationships that could have appeared to influence the work reported in this paper.

Acknowledgement

I would like to thank all authors for their contributions. Studies were carried out in the Inonu University Molecular Biology and Genetic Cell Culture Laboratory. This study was supported by Inonu University Research Project Unit (Project No: I.U.BAP 2016/154). This work is part of Işıl Yıldırım's doctoral dissertation. The authors acknowledge Dokuz Eylül University for the use of the Rigaku Oxford Xcalibur Eos Diffractometer (purchased under University Research Grant No. 2010.KB•FEN.13).

Supplementary materials

Supplementary material associated with this article can be found, in the online version, at doi:10.1016/j.molstruc.2020.129462.

References

- [1] (2019). <http://www.WHO.com>.
- [2] (2019). https://www.breastcancer.org/symptoms/understand_bc/statistics, <https://www.fda.gov/newsevents/newsroom/pressannouncements/ucm567309.htm>.
- [3] (2020). <https://seer.cancer.gov/statfacts/html/breast.html>.
- [4] U. Kalinowska-Lis, A. Felczak, L. Checinska, I. Szablowska-Gadomska, E. Patyna, M. Malecki, K. Lisowska, J. Ochocki, Antibacterial activity and cytotoxicity of silver(I) complexes of pyridine and (Benz)imidazole derivatives. X-ray crystal structure of [Ag(2,6-di(CH₂OH)py)₂INO₃], *Molecules* 21 (2) (2016) 87. [10.3390/molecules21020087](https://doi.org/10.3390/molecules21020087).
- [5] C.H. Wang, W.C. Shih, C.H. Chang, Y.Y. Kuo, W.C. Hung, T.W. Ong, W.S. Li, Preparation and characterization of amino-linked heterocyclic carbene palladium, gold, and silver complexes and their use as anticancer agents that act by triggering apoptotic cell death, *J. Med. Chem.* 54 (2011) 5245–5249, doi:10.1021/jm101096x.
- [6] R.A. Haque, S.F. Nasri, M.A. Iqbal, S. Al-Rawi, S.F. Jafari, M.B.K. Ahamed, A. Majid, Synthesis, characterization, and crystal structures of bis-imidazolium salts and respective dinuclear Ag (I) N-heterocyclic carbene complexes: in vitro anticancer studies against "human colon cancer" and "breast cancer", *Hindawi Publ. Corp. J. Chem.* 2013 (2013) 1–11, doi:10.1155/2013/804683.
- [7] W. Streciwilk, J. Cassid, F. Hackenberg, H. Müller Bunz, F. Paradisi, M. Tacke, Synthesis, cytotoxic and antibacterial studies of p-benzyl-substituted NHC-silver(I) acetate compounds derived from 4,5-di-pdiisopropylphenyl-or 4,5-di-p-chlorophenyl-1H-imidazole, *J. Organomet. Chem.* 749 (2014) 88–99, doi:10.1016/j.jorganchem.2013.09.033.
- [8] M.A. Iqbal, R.A. Haque, M.B.K. Ahamed, M.A. Abdul, S. Al-Rawi, Synthesis and anticancer activity of para-xylyl linked bis-benzimidazolium salts and respective Ag(I)-Nheterocyclic carbene complexes, *Med. Chem. Res.* 22 (5) (2013) 2455–2466, doi:10.1007/s00044-012-0240-6.
- [9] C. Graham, The role of silver in wound healing, *J. Nurs.* 14 (19) (2005) 22–24, doi:10.12968/bjon.2005.14.Sup5.19954.
- [10] A. Kascatan-Nebioglu, M.J. Panzner, C.A. Tessier, C.L. Cannon, W.C. Youngs, N-Heterocyclic carbene-silver complexes: a new class of antibiotics, *Coord. Chem. Rev.* 251 (5–6) (2007) 884–895, doi:10.1016/j.ccr.2006.08.019.
- [11] R.A. Haque, M.A. Iqbal, M.B. Khadeer Ahamed, A.A. Majid, Z.A. Abdul Hameed, Design, synthesis and structural studies of meta-xylyl linked bis-benzimidazolium salts: potential anticancer agents against 'human colon cancer', *Chem. Cent.* 6 (1) (2012) 68, doi:10.1186/1752-153X-6-68.
- [12] R.A. Haque, M.Z. Ghdhayeb, S. Budagumpi, A. Salman, M.B. Khadeer Ahamed, A.M.S. Abdul Majid, Non-symmetrically substituted N-heterocyclic carbene-Ag(I) complexes of benzimidazol-2-ylidenes: synthesis, crystal structures, anticancer activity and transmetalation studies, *Inorg. Chim. Acta* 394 (1) (2012) 519–525, doi:10.1016/j.ica.2012.09.013.
- [13] M.A. Iqbal, R.A. Haque, S. Budagumpi, M.B. Khadeer Ahamed, A.M.S. Abdul Majid, Short metal-metal separations and in vitro anticancer studies of a new dinuclear silver(I)-N-heterocyclic carbene complex of para-xylyl-linked bis-benzimidazolium salt, *Inorg. Chem. Commun.* 28 (2013) 64–69, doi:10.1016/j.inoche.2012.11.013.
- [14] M.A. Iqbal, R.A. Haque, M.B.K. Ahamed, A. Majid, S.S. Al-Rawi, Synthesis and anticancer activity of para-xylyl linked bis-benzimidazolium salts and respective Ag(I)- Nheterocyclic carbene complexes, *Chem. Res.* 22 (2013) 2455–2466, doi:10.1007/s00044-012-0240-6.
- [15] E.C. Friedberg, G.C. Walker, W. Siede, R.D. Wood, DNA Repair and Mutagenesis, American Society for Microbiology Press, Washington, USA, 2005.
- [16] I. Yıldırım, A. Aktas, D. Barut-Celepci, S. Kirbağ, T. Kutlu, Y. Gök, M. Aygün, Synthesis, characterization, crystal structure, and antimicrobial studies of 2-morpholinoethyl-substituted benzimidazolium salts and their silver(I)-N-heterocyclic carbene complexes, *Res. Chem. Intermed.* 43 (11) (2017) 6379–6393, doi:10.1007/s11164-017-2995-3.
- [17] CrysAlisPro Software System, Rigaku Oxford Diffraction, 2019.
- [18] G.M. Sheldrick, SHELXT - integrated space-group and crystal-structure determination, *Acta Crystallogr. Sect. A* 71 (2015) 3–8, doi:10.1107/S2053273114026370.
- [19] O.V. Dolomanov, L.J. Bourhis, R.J. Gildea, J.A.K. Howard, H. Puschmann, OLEX2: a complete structure solution, refinement and analysis program, *J. Appl. Cryst.* 42 (2009) 339–341, doi:10.1107/S0021889808042726.
- [20] G.M. Sheldrick, Crystal structure refinement with SHELXL, *Acta Crystallogr. Sect. C* 71 (2015) 3–8, doi:10.1107/S2053229614024218.
- [21] M.V. Berridge, A.S. Tan, Characterization of the cellular reduction of 3-(4,5-dimethylthiazol-2-yl)-2,5-diphenyltetrazolium bromide (MTT): subcellular localization, substrate dependence, and involvement of mitochondrial electron transport in MTT reduction, *Arch. Biochem. Biophys.* 303 (1993) 474–482.
- [22] (2008). <http://www.bdbiosciences.com/ds/pm/tds/556547.pdf>.
- [23] M. Dikmen, Z. Cantürk, Y. Öztürk, Y.I. Tunali, Investigation of the apoptotic effect of curcumin in human leukemia HL-60 cells by using flow cytometry, *Cancer Biother. Radiopharm.* 25 (6) (2011) 749–755. [10.1089/cbr.2010.0822](https://doi.org/10.1089/cbr.2010.0822).
- [24] (2015). <http://www.bdbiosciences.com/ds/is/tds/23-2923.pdf>.
- [25] (2015). <http://www.bdbiosciences.com/ds/pm/tds/550480.pdf>.
- [26] A. Aktas, D. Barut Celepci, Y. Gök, Synthesis, crystal structures, spectral FT-IR, NMR and UV-vis investigations and Hirshfeld surface analysis of two new 2-hydroxyethyl-substituted N-heterocyclic carbene precursors, *J. Chin. Chem. Soc.* 66 (10) (2019) 1389–1396, doi:10.1002/jccs.201900020.
- [27] W. Liu, K. Bendorf, A. Hagenbach, U. Abram, B.A. Niu, A. Maripapan, R. Gust, Synthesis and biological studies of silver N-heterocyclic carbene complexes derived from 4,5-diarylimidazole, *Eur. J. Med. Chem.* 46 (12) (2011) 5927–5934, doi:10.1016/j.ejmech.2011.10.002.
- [28] S. Akkoç, İ.Ö. İlhan, Y. Gök, P.J. Upadhyay, V. Kayser, In vitro cytotoxic activities of new silver and PEPSI palladium N-heterocyclic carbene complexes derived from benzimidazolium salts, *Inorg. Chim. Acta* 449 (2016) 75–81, doi:10.1016/j.ica.2016.05.001.
- [29] S.Y. Hussain, R.A. Haque, P.O. Asekunowo, A.M.S. Abdul Majid, M.T. Agha, M.R. Razalli, Synthesis, characterization and anti-proliferative activity of propylene linked bis-benzimidazolium salts and their respective dinuclear silver(I)-N-heterocyclic carbene complexes, *J. Organomet. Chem.* 840 (2017) 56–62, doi:10.1016/j.jorganchem.2017.04.011.
- [30] E. Çevik-Yıldız, N. Şahin, S. Şahin-Bölükbaşı, Synthesis, characterization and investigation of antiproliferative activity of novel Ag(I)-heterocyclic carbene (NHC) complexes, *J. Mol. Struct.* 1199 (2020) 126987, doi:10.1016/j.molstruc.2019.126987.
- [31] A.M. Otto, R. Paddenberg, S. Schubert, H.S. Mannherz, Cell-cycle arrest, micronucleus formation, and cell death in growth inhibition of MCF-7 breast cancer cells by tamoxifen and cisplatin, *J. Cancer Res. Clin. Oncol.* 122 (1996) 603–612, doi:10.1007/BF01221192.
- [32] R.U. Jänick, M.L. Sprengart, M.R. Wati, A.G. Porter, Caspase-3 is required for DNA fragmentation and morphological changes associated with apoptosis, *J. Biol. Chem.* 273 (1998) 9357–9360, doi:10.1074/jbc.273.16.9357.
- [33] O. Kutuk, E.D. Arisan, T. Tezil, M.C. Shoshan, H. Basaga, Cisplatin overcomes Bcl-2-mediated resistance to apoptosis via preferential engagement of Bak: critical role of Noxa-mediated lipid peroxidation, *Carcinogenesis* 30 (9) (2009) 1517–1527, doi:10.1093/carcin/bgp165.
- [34] A. Habib, V.M. Nazari, M.A. Iqbal, H.N. Bhatti, M.B.K. Ahmed, A.M.S.A. Majid, Unsymmetrically substituted benzimidazolium based silver(I)-N-heterocyclic carbene complexes: synthesis, characterization and in vitro anticancer study against human breast cancer and colon cancer, *J. Saudi Chem. Soc.* 23 (7) (2019) 795–808, doi:10.1016/j.jscs.2019.03.002.